JACS
JOURNAL OF THE AMERICAN CHEMICAL SOCIETY
Article
pubs.acs.org/JACS

From Molecules to Surfaces: Radical-Based Mechanisms of Si–S and Si–Se Bond Formation on Silicon

Jillian M. Buriak* and Md Delwar H. Sikder

Department of Chemistry, University of Alberta, and the National Institute for Nanotechnology, Edmonton, AB T6G 2G2, Canada

Supporting Information

ABSTRACT: The derivatization of silicon surfaces can have profound effects on the underlying electronic properties of the semiconductor. In this work, we investigate the radical surface chemistry of silicon with a range of organochalcogenide reagents (comprising S and Se) on a hydride-terminated silicon surface, to cleanly and efficiently produce surface Si–S and Si–Se bonds, at ambient temperature. Using a diazonium-based radical initiator, which induces formation of surface silicon radicals, a group of organochalcogenides were screened for reactivity at room temperature, including di-*n*-butyl disulfide, diphenyl disulfide, diphenyl diselenide, di-*n*-butyl sulfide, diphenyl selenide, diphenyl sulfide, 1-octadecanethiol, *t*-butyl disulfide, and *t*-butylthiol, which comprises the disulfide, diselenide, thiol, and thioether functionalities. The surface reactions were monitored by transmission mode Fourier transform infrared (FTIR) spectroscopy, X-ray photoelectron spectroscopy, and time-of-flight secondary ionization mass spectrometry. Calculation of Si–H_x consumption, a semiquantitative measure of yield of production of surface-bound Si–E bonds (E = S, Se), was carried out via FTIR spectroscopy. Control experiments, *sans* the BBD diazonium radical initiator, were all negative for any evident incorporation, as determined by FTIR spectroscopy. The functional groups that did react with surface silicon radicals included the dialkyl/diphenyl disulfides, diphenyl diselenide, and 1-octadecanethiol, but not *t*-butylthiol, diphenyl sulfide/selenide, and di-*n*-butyl sulfide. Through a comparison with the rich body of literature regarding molecular radicals, and in particular, silyl radicals, reaction mechanisms were proposed for each. Armed with an understanding of the reaction mechanisms, much of the known chemistry within the extensive body of radical-based reactivity has the potential to be harnessed on silicon and could be extended to a range of technologically relevant semiconductor surfaces, such as germanium, carbon, and others.

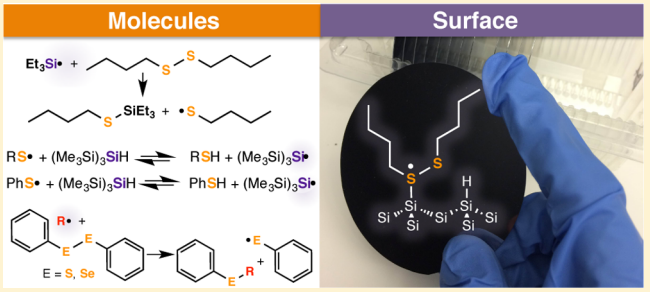

INTRODUCTION

The functionalization of silicon surfaces is of interest for applications that range from integration of biomolecules with silicon-based devices[1] and modulation of the electronic properties of bulk and nanocrystalline silicon-based structures[2,3] and for development of molecular electronics-on-silicon[4−7] and silicon-based devices for solar energy conversion,[8] among many others.[9−12] The most widely used approaches for derivatizing the surface of silicon involve the formation of Si–H bonds (hydride termination),[13−17] ≡Si–O bonds (oxidation and silyl ether linkages),[18−21] ≡Si–Cl bonds,[22,23] and ≡Si–C bonds (via reactions such as hydrosilylation).[24−32] The nature of the linkage to the surface, including bond length and dipole, can have profound effects on electronic properties of the underlying silicon,[33−37] including modulation of work function,[38−40] introduction of surface states of varying energies,[41] as well as affecting the packing of an overlying organic monolayer in the case of molecular adsorbates.[37,42] The band edges of a semiconductor are highly sensitive to the nature of the bound surface molecules,[37] and thus choice of surface termination is important. When considering nanocrystalline versions of silicon,[43] including porous silicon, silicon nanowires, and colloidal silicon nanocrystals, the ratio of surface atoms to bulk is high, and thus the effect of the exogenous atoms to which surface silicon atoms are bound could be of even greater significance.[1,44] Surface functionalization can passivate defects such as dangling bonds, which has dramatic effects on photoluminescence,[45,46] and can affect and hence modulate the band gap of quantum confined silicon.[47−49]

Unlike widely studied ≡Si–O bond formation, chemistry of oxygen's chalcogenide cousins, ≡Si–E bonds (E = S, Se), has seen far less attention.[50] ≡Si–S and ≡Si–Se bonds could be of interest, for instance, if an electrochemically active interface is desired in a surface-bound monolayer: The nature of the bond to the silicon is important due to factors arising from the bond length and availability of additional electronic states, in the case of a heavier atom (S, Se versus O).[37,51] From a fundamental perspective, the chemistry of organochalcogenides on silicon surfaces has not been extensively investigated and could offer a rich and diverse repertoire of reactivity, as is seen in the case of molecular organosilane chemistry.[52−54]

Received: June 3, 2015
Published: July 10, 2015

DOI: 10.1021/jacs.5b05738
J. Am. Chem. Soc. 2015, 137, 9730−9738

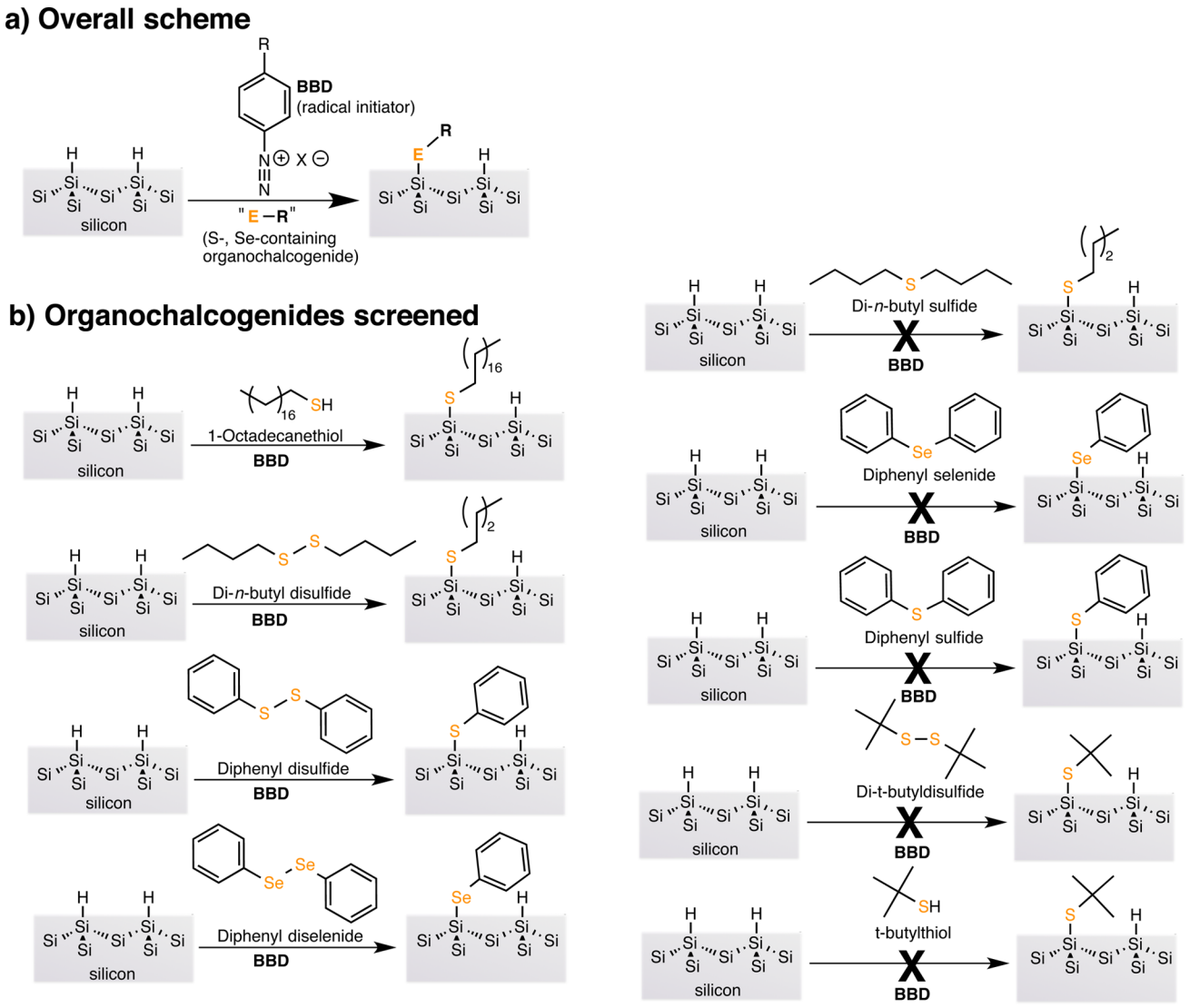

Figure 1. (a) Overall reaction outlining the chemistry screened in this paper. The diazonium salt, BBD, was used as a radical initiator on the hydrogen-terminated porous silicon surface. (b) The nine organochalcogenide molecules that were screened for reactivity under radical conditions (BBD as the initiator) on hydrogen-terminated porous silicon.

While UHV results leading to ≡Si–E (E = S, Se) bond formation on silicon surfaces date back to the 1980s,[55−60] to the best of our knowledge, the earliest example of wet chemical ≡Si–S and ≡Si–Se bond formation on silicon surfaces was published by Bocian and co-workers in 2003; this group showed that acetylchalcogenidoarene-derivatized (Ar-EAc, E = O, S, Se) porphyrins could be covalently linked to Si(100)–H_x surfaces through ≡Si–O, ≡Si–S, and ≡Si–Se bonds using a short, but high temperature (400 °C), annealing step.[50,51] Later, a wet-chemical functionalization strategy for Si–E formation on silicon (E = S) was demonstrated to occur upon UV irradiation of long chain aliphatic thiols on hydride-terminated Si(100) surfaces,[61] a result that was followed up on Si(111)–H surfaces;[62] the reaction mechanism that was proposed proceeded via homolytic cleavage of the ≡Si–H bond to yield the reactive surface-bound ≡Si• species.[62,63] In separate works, Hacker[64] and Sugimura and co-workers[65] demonstrated that heating of a Si(111)–H surface in a solution of a long-chain aliphatic thiol in the high boiling point solvent, mesitylene, at 150 °C resulted in formation of self-assembled monolayers with high water contact angles. The authors proposed a mechanism based upon nucleophilic attack on a surface silicon atom to produce a ≡Si–S bond and H_2, although this proposal was not substantiated with further data.

Silicon surface radicals have long been implicated in surface functionalization, starting with Chidsey's landmark thermally driven hydrosilylation chemistry.[24,25] In earlier work, we showed that diazonium reagents could act as radical initiator on hydrogen-terminated silicon surfaces, at room temperature, to produce surface ≡Si• radicals that could be harnessed for further functionalization.[66] 4-bromobenzenediazonium tetrafluoroborate, here abbreviated as BBD, cleanly initiated hydrosilylation of alkenes and alkynes at room temperature on porous silicon, leading to alkyl- and alkenyl-terminated functionalities, respectively (Figure 1a). The reaction was consistent with a radical mechanism, in which surface silicon radicals were trapped by a high concentration of alkene/alkyne, leading to a range of functional alkyl monolayers on the surface; similar hydrosilylation chemistry had been described with molecular R_3Si• radicals, in the presence of alkene/alkynes.[52,54,67] In an attempt to substantiate the involvement of silicon surface radical intermediates, it was demonstrated that

DOI: 10.1021/jacs.5b05738
J. Am. Chem. Soc. 2015, 137, 9730−9738

the selenium ether, ethylphenylselenide, resulted in surface-bound ≡Si−Se−Ph functionalities,[66] a reaction that could conceivably only occur through silyl radical trapping via a seleranyl radical intermediate, as has been documented with molecular $R_3Si\bullet$ radicals and alkylarylselenides, ArSeR.[52,67] Molecular chemistry of $R_3Si\bullet$ radicals with ethylphenylsulfide, EtSPh in solution, is, however, much slower,[67] and similarly on porous silicon, no ≡Si−S−Ph bond formation was noted under these conditions.[66] No further diazonium-mediated silicon surface chemistry was carried out with chalcogenide compounds, and thus little is known about reaction scope, mechanism, and quantification of yields/efficiency. Intrigued by the possibility of enabling facile, efficient, and room-temperature formation of ≡Si−ER groups on silicon, we set out to investigate the reaction space of this chemistry, with the goal of elucidating the mechanistic pathway(s), and to establish a practical route to organochalcogenide-functionalized silicon interfaces. Control of the surface functionalization could be extremely useful for applications in the areas of molecular-silicon integration, and control of the electronic properties of nanoscale silicon materials. In this work, we examined the reactivity of a range of organochalcogenide compounds with porous silicon and arrived at likely mechanisms by drawing connections with molecular silane chemistry.

RESULTS

In this work, we screened the reactivity of nine different organochalcogenide compounds (containing S, Se atoms) on hydride-terminated porous silicon surfaces, in the presence of the diazonium-based radical initiator, BBD, as shown schematically in Figure 1a. Diaryl- and dialkylchalcogenides and diaryl- and dialkyldichalcogenides as well as thiols were screened under room temperature conditions, as summarized in Figure 1. In all cases, a large excess of the chalcogenide compound was used to favor trapping of the presumed surface silicon radical to result in ≡Si−ER formation (E = S, Se), over grafting of the $-C_6H_5Br$ aryl group derived from the diazonium initiator, BBD.[68] It was observed that of the nine compounds, only four resulted in clean formation of ≡Si−ER bonds, while the other five showed little-to-no spectroscopic evidence for surface chalcogenide functionalization; in these cases, only coupling of the $-C_6H_5Br$ group and concomitant oxidation due to residual water and/or oxygen was the major product (*vide infra*). As has been shown previously, the reaction of porous silicon with BBD, in absence of a radical trap such as an alkene or a reactive chalcogenide, leads to grafting of $-C_6H_5Br$ aryl groups and substantial oxidation of the surface surface.[66]

The high surface area of porous silicon, with its good transmission profile with respect to infrared irradiation, allows for clean analysis of the reaction products on the surface by Fourier transform infrared (FTIR) spectroscopy.[26,69] Figure 2 shows transmittance FTIR spectra for porous silicon samples before and after reaction with different organochalcogenides, with accompanying exposure to the diazonium-based initiator, BBD. The left-hand spectra show the full mid-IR range, and the spectra on the right show the $\nu(SiH_x)$ stretching feature before and after reaction to semiquantify the consumption of SiH_x bonds. The FTIR spectrum of freshly prepared porous silicon is dominated by surface hydride features from the $\nu(Si-H_x)$ stretches centered around 2100 cm^{-1} and lower energy bending modes, $\delta(Si-H_x)$, just above 800 cm^{-1} (Figure 2a,b). Following treatment for 2 h with 1-octadecanethiol and the diazonium initiator, BBD, obvious $C-H_x$ stretches that

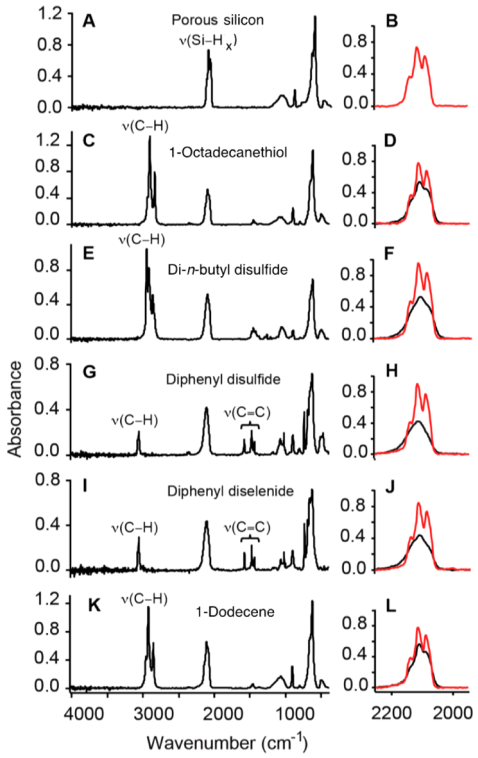

Figure 2. FTIR spectra (transmission mode) of porous silicon samples before, and after, reaction with the reagent indicated, in the presence of the diazonium initiator, BBD. The spectra on the left show the full mid-IR range, and the spectra on the right show the $\nu(Si-H_x)$ region before reaction (red curve) and after reaction (black).

correspond to the profile of an octadecyl chain appear just below 3000 cm^{-1} (Figure 2c), accompanied by diminished intensity of the $\nu(Si-H_x)$ features (Figure 2d), pointing to consumption of silicon−hydride bonds. Little surface silicon oxidation took place, as shown by the lack of change of the broad $\nu(Si-O)$ feature around 1100 cm^{-1}.[18] Other species that react cleanly with BBD initiation on porous silicon include di-*n*-butyldisulfide (Figure 2e,f), diphenyl disulfide (Figure 2g,h), and diphenyl diselenide (Figure 2i,j). The spectrum corresponding to BBD-initiated hydrosilylation of 1-dodecene is shown in Figure 2k,l for comparison. Control experiments carried out with all nine of these organochalcogenide compounds, in absence of BBD, showed no change in the FTIR spectrum of the porous silicon.

Using the integrated intensity of the $\nu(Si-H_x)$ modes in the spectra on the right-hand side of Figure 2, a semiquantitative analysis of consumption of $Si-H_x$ groups can be carried out, as per eq 1:[70,72]

$$\text{Surface coverage in\%} = \frac{(A_{\text{Si–H(before)}} - A_{\text{Si–H(after)}}) \times 100}{A_{\text{Si–H(before)}}} \quad (1)$$

where A is the area of the integrated intensity of the absorption of the specified feature. A summary of calculated hydride consumption can be found in Table 1. The aliphatic thiols [1-octanethiol is shown in the Supporting Information (SI)] result in consumption of ∼15% of the $Si-H_x$ groups, whereas the disulfides and diselenides lead to consumption of ∼27−35% of the $Si-H_x$ bonds on the surface, with the latter values on par with hydrosilylation results on porous silicon surfaces.[69,71] In

DOI: 10.1021/jacs.5b05738
J. Am. Chem. Soc. 2015, 137, 9730−9738

Table 1. Calculated Hydride Consumption[a]

reagent	% decrease of ν(Si−H_x) intensity (FTIR)
1-octadecanethiol	15 ± 1
1-octanethiol	14 ± 1
di-*n*-butyl disulfide	27 ± 1
diphenyl disulfide	35 ± 7
diphenyl diselenide	29 ± 1
1-dodecene	12 ± 4

[a]Averages calculated from three separate experiments. " ± " Values represent upper and lower limits of the average.

this work, 1-dodecene, which undergoes hydrosilylation to form ≡Si−$C_{12}H_{25}$ groups on the surface, has been included as a comparison, using the same concentration and contact time as that used for the organochalcogenides. Previously, BBD-initiated hydrosilylation of 1-dodecene was shown to reduce Si−H_x intensity by ∼28%, but in this work, we only observed substitution of 12 ± 4% as a result of the shorter contact time, 2 h versus 3 h, and dilution of the alkene.[66] The results are suggestive of higher reactivity of the disulfides and diselenides under these conditions, compared to hydrosilylation of 1-dodecene under the same conditions. Based upon the FTIR data, a full summary of the proposed reactivity of the organochalcogenide reagents with porous silicon is provided in Figure 1. The five reagents that did not lead to FTIR spectra with features corresponding to those of the organochalcogenide groups are shown with an 'X' through the reaction arrow; the FTIR spectra of these porous silicon samples are shown in the SI and are dominated by oxidation.

X-ray photoelectron spectroscopy (XPS) of BBD-initiated reactions of porous silicon with 1-octadecanethiol, diphenyl disulfide, diphenyl diselenide, and di-*n*-butyl disulfide is shown in Figure 3. The Si(2p) spectra of all four porous silicon samples reveal no significant oxidation, which would appear due to oxygen insertion into surface Si−Si and Si−H_x bonds, resulting in features with higher binding energies of the order of >101 eV.[72] The S(2p) spectra show the characteristic doublet centered around ∼163 eV,[60] while the Se(2p) spectrum corresponds to a doublet centered at ∼55.5 eV, which agrees with previous results by Bocian on porphyrin monolayers bound through Si−Se bonds on Si(100) surfaces.[50,51] To complement the XPS data, time-of-flight depth profiling [time-of-flight secondary ionization mass spectrometry (ToF-SIMS)] of the porous silicon samples was carried out to provide additional data regarding coverage. Unlike XPS, which can only sample the top layers of the porous silicon, depth profiled ToF-SIMS provides relative compositions throughout the entire porous structure, from the top of the film through to the underlying bulk silicon.[66,73] When compared to an unfunctionalized porous silicon sample that had been etched under identical conditions, ToF-SIMS can be used to compare the quantity, in counts, of a specific atom of interest. As shown in Figure 4, for 1-octadecanethiol, di-*n*-butyl disulfide, diphenyl disulfide, and diphenyl diselenide, the relative quanitities of carbon in the functionalized porous silicon are at least 1 order of magnitude higher than the levels of adventitious carbon found in an unfunctionalized sample of porous silicon (Figure 4b,d,f,h). For the sulfur-containing organochalcogenides, the quantity of sulfur in the film is 1−2 orders of magnitude higher than the unfunctionalized comparison (Figure 4a,c,e), while the difference for the selenium compound is even more dramatic (Figure 4g). In addition, the relative quantities of the atoms of interest (S, Se, C) in the functionalized samples appear consistent throughout the film, suggesting even coverage throughout the porous silicon matrix.

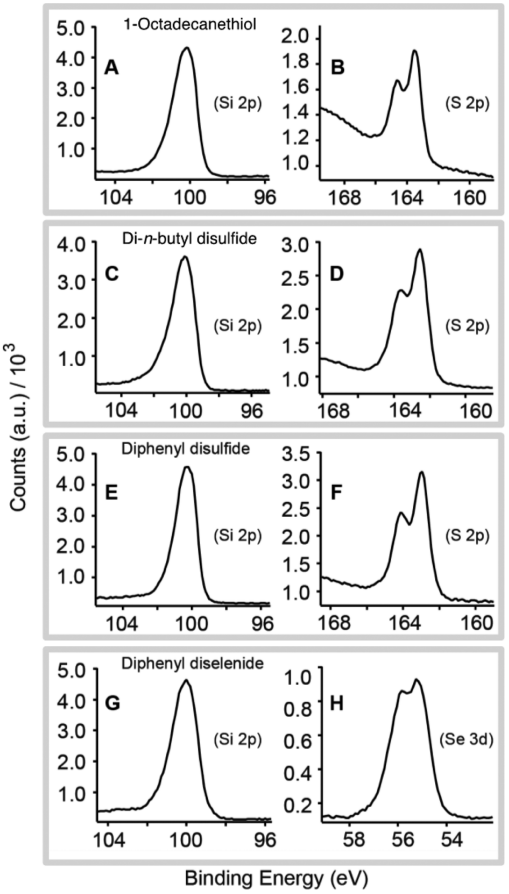

Figure 3. XPS of porous silicon samples before and after reaction with the reagent indicated, in the presence of the diazonium initiator, BBD.

DISCUSSION

Since control experiments showed no reaction between any of the organochalcogenide reagents tested in absence of the BBD initiator under these conditions, consideration of the mechanism starts with the reactivity of BBD with porous silicon, as shown in Figure 5a. As an electrophilic diazonium reagent, BBD is reduced by the silicon, leading to decomposition and formation of a bromoaryl radical and release of N_2.[66,68] The resulting positive charge on the silicon surface may be neutralized via release of HBF_4 and formation of a surface Si radical.[66,74] Since the starting point of the reaction appears to be a surface-bound ≡Si• group, the molecular chemistry of organochalcogenides with silyl radicals should lead to mechanistic insights. Molecules containing S-[75−77] and Se-[78−80] based substituents are well-established players in radical chemistry, including the molecular chemistry of silyl radicals.[52,67,81] A summary of representative radical reactions used to buttress the proposed surface-based mechanisms is shown in Table 2.

Proposed mechanisms to explain the observed surface reactivity of Si−H_x-terminated surfaces with these chalcognide molecules are shown in Figures 5−7. Starting with the reaction of di-*n*-butyl disulfide with porous silicon upon BBD initiation, shown in Figure 5b, spectroscopic data (*vide supra*) points to ≡Si−S-*n*-Bu termination. It was shown almost 30 years ago by

DOI: 10.1021/jacs.5b05738
J. Am. Chem. Soc. 2015, 137, 9730−9738

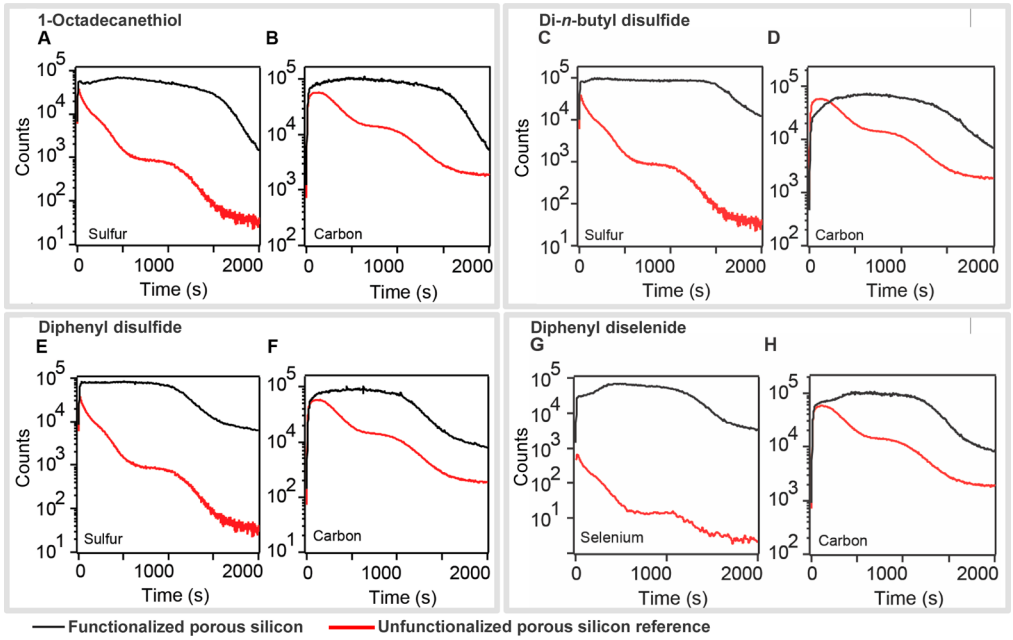

Figure 4. ToF-SIMS analysis of porous silicon samples. The black curves represent the porous silicon samples after reaction with the reagent indicated in the presence of the diazonium initiator, BBD. The same sample of unfunctionalized porous silicon was used as the comparison (reference sample, red line) in all four spectra.

Platz and co-workers that the homolytic displacement reaction of the silyl radical $Et_3Si\bullet$ with di-*n*-butyl disulfide, BuSSBu, proceeds via release of the *n*-butyl thiyl radical and formation of an Si−S bond in the resulting product (Table 2, entry 1);[82] the reaction proceeds almost 100 times faster than the reaction with di-*n*-butyl sulfide, BuSBu, shown in Table 2, entry 2. The reasons proposed for the much higher reactivity of BuSSBu versus BuSBu were the lower bond dissociation energy of the S−S bond versus the S−C bond (53−57 and 74 kcal/mol, respectively) and the longer S−S bond, which could lead to decreased steric encumbrance.[82] Thus, on the silicon surface, the formed ≡Si• could engage in similar homolytic displacement, forming the ≡Si−SBu termination on the surface. Similarly, reactions of alkyl radicals with diaryl disulfides and diselenides, entry 3 in Table 2, are also well-known in the context of using these molecules as radical traps, with the reactivity of PhSeSePh being 160 times faster than PhSSPh as an alkyl radical trap R•.[83−85] A similar mechanism, shown in Figure 5c, was postulated to occur on between surface silicon radicals and PhSeSePh and PhSSPh. The only RSSR molecule that did not lead to obvious incorporation by FTIR was di-*t*-butyl disulfide, *t*-BuSS(*t*-Bu), Figure 5b. Presumably, steric hindrance between the bulky *t*-butyl group on the sulfur undergoing the S_H2 addition and the surface prevented the reaction from proceeding. Platz and co-workers concluded that with regards to $Et_3Si\bullet$ addition to various sulfide compounds, the kinetics of the reaction are more sensitive to sterics than to stability of the product (ie, bond strengths), which could be the case on the surface as well.[82]

In the case of sulfides and selenides of the form PhER (R = alkyl, E=S, Se), Chatgilialoglu and co-workers examined the reactivity of these molecules with the molecular silyl radicals, $(Me_3Si)_3Si\bullet$ and $Et_3Si\bullet$.[52,67] The reaction with $PhSeC_{10}H_{21}$ resulted in the fast formation of a seleranyl radical intermediate upon addition of the silyl radical, followed by collapse to produce ≡Si−SePh molecules upon *α*-cleavage of the Se−C_{alkyl} bond (entry 4, Table 2); the same reaction with the selenium variant, $PhSeC_{10}H_{21}$, as mentioned earlier, was at least an order of magnitude slower.[67] It is the E−C_{alkyl} bond that is cleaved since the C_{sp^3}−E bond is weaker than the phenyl C_{sp^2}−E bond (E = S, Se).[86] The mechanism proposed, as shown in Figure 6, is a stepwise S_H2 mechanism, involving binding of the arylalkyl thio- or selenoether with the silyl radical, to produce the intermediate sulfuranyl or seleranyl intermediate, followed by *α*-cleavage to lead to the final products.[52,67] None of the reactions with chalcogenide ethers, di-*n*-butyl sulfide (BuSBu), diphenylsulfide (PhSPh), or disphenylselenide (PhSePh) resulted in incorporation of alkyl/aryl features with porous silicon that corresponded with the expected ≡Si−ER products, as shown by FTIR spectroscopy (E = S, Se; SI). Earlier work from our group in 2006 showed that phenylethylselenide, PhSeEt, did result in ≡Si−SePh incorporation, whereas phenylethylsulfide, PhSEt, did not, as shown in Figure 6b,c.[66] These results mirror the known reactivity of silyl molecules, which showed that the propensity of the seleno derivative to undergo *α*-cleavage of the Se−C_{alkyl} bond in molecules was much higher in the selenium derivatives, as opposed to the sulfur variants.[52,67,82]

The last type of molecule that was shown to react with the surface and produce ≡Si−SR groups was alkanethiols. The proposed mechanism is shown in Figure 7a and is a variant of the stepwise S_H2-based mechanism described for thioethers (Figure 6). Another mechanism that could be postulated is that of a free thiyl radical in solution combining with a surface silyl radical, as has been suggested previously for thermally driven thiol monolayer formation on Si(111)−H:[62,63]

$$RS\bullet + \equiv Si\bullet \rightarrow \equiv Si{-}SR$$

Looking within the vast literature regarding combinations of silanes and thiols under radical conditions (typically for organic reduction and coupling reactions), observation of ≡Si−SR products and/or intermediates is not, to the best of our knowledge, typical. The only example from the molecular literature we could find was a high temperature reaction

DOI: 10.1021/jacs.5b05738
J. Am. Chem. Soc. 2015, 137, 9730−9738

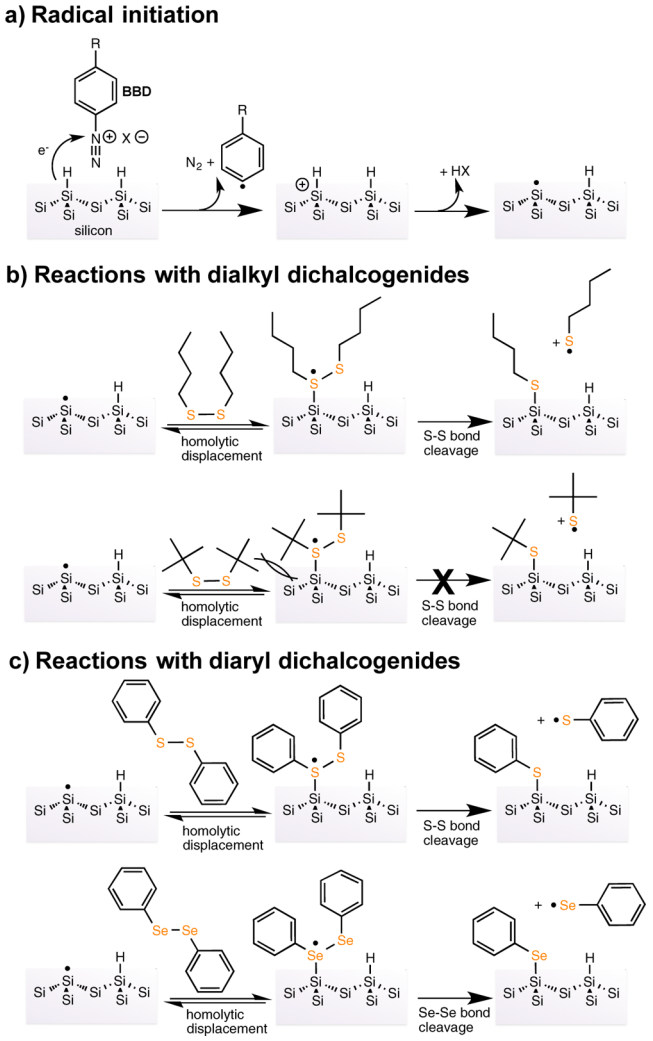

Figure 5. (a) Reaction of the diazonium reagent, BBD, with a hydride-terminated silicon surface. (b) Proposed homolytic displacement mechanism for the reaction of dialkyl disulfides with a silicon-surface radical. (c) Proposed homolytic displacement mechanism for the reaction of diphenyl disulfide and diphenyl diselenide with silicon-surface radicals.

between triphenylsilane and p-thiocresol, which resulted in formation of triphenyl-(*p*-tolylthio)-silane.[87] The H-exchange equilibria between thiols and silanes, under radical conditions (shown in Table 2, entry 5) are, however, well-studied and have considerable precedent.[79,88−90] The equilibrium with RSH (R = alkyl) is slightly exothermic by approximately −3.5 kcal/mol and slightly endothermic by 5.0 kcal/mol when R is phenyl.[88] Because the reaction on the porous silicon surface is carried out with a large excess of thiol, we would assume that [RS•] in the solution phase would be low when compared to [RSH]. We also noted that the reaction with *t*-butylthiol did not lead to ≡Si−S-*t*-Bu termination, which suggests that steric hindrance dominates, a result that correlates with previous observations.[82] While still unsettled, the lack of reactivity of *t*-butylthiol and the known stepwise S_H2 mechanism for related organochalcogenides suggests that the reaction proceeds via the radical intermediate shown in Figure 7a, although we cannot rule out direct coupling of RS• to surface ≡Si• species.[87] The lower substitution level of the alkanethiol as measured by consumption of surface Si−H_x groups, when compared to the disulfides/diselenides (Figures 2c-d, and Table 1), could be due to the competing hydrogen addition equilibria, shown in Figure 7b, in which the surface-bound ≡Si• radical abstracts H• from RSH in solution; this competing reaction lowers the amount of ≡Si−SR bond formation on the silicon surface.[88−90]

■ CONCLUSIONS

In contrast to ≡Si−C bond formation via hydrosilylation on silicon surfaces, which has been heavily studied and applied,[91] other linkages have been shown to result in intriguing electronic effects,[3,37] and computational work has suggested that they could provide control over the underlying electronics of the silicon semiconducting material, particularly at the nanoscale.[37] In order to provide reaction schemes on silicon surfaces that enable clean and efficient access to different functionalities and chemical bonding motifs, the surface reactivity of silicon requires further elucidation. There is demand for room-temperature chemical methods, particularly when the chemistry involves fragile nanoscale materials or thermally sensitive molecules (i.e., biomolecules). Here we described a rapid, room-temperature, high-substitution approach to enabling the formation of Si−S and Si−Se bonds and propose radical-based pathways as the most probable mechanistic framework. Connections to the molecular silyl radical literature were made, and the resulting chemical reactivity patterns on the silicon surface were shown to mirror those of the corresponding molecular systems. Because the radical chemistry of main group species is so rich, there is vast potential to build bonds based upon Si−E linkages on silicon, where E could include, for example, Te, P, As, Sn, and to expand to the surfaces of other technologically interesting materials, such as carbon, germanium, and others.

■ EXPERIMENTAL SECTION

General. Diphenyl disulfide (99%), diphenyl diselenide (98%), di-*n*-butyl disulfide (97%), diphenyl sulfide (98%), diphenyl selenide (96%), di-*n*-butyl sulfide (≥95%), 1-dodecene (≥99%), 1-octanethiol (≥98.5%), di-*t*-butyl disulfide (97%), *t*-butylthiol (2-methyl-2-propanethiol, 99%), 1-octadecanethiol (98%), 4-bromodiazonium tetrafluoroborate (96%), aluminum oxide (activated, neutral, Brockmann I, standard grade, ~150 mesh, 58 Å, dried for >24 h in a 100 °C oven and taken into an argon atmosphere glovebox while still hot), and dry acetonitrile (SureSeal bottle) were purchased from Sigma-Aldrich. All reagents were stored at −20 °C inside the inert atmosphere of an argon-filled glovebox. HF 49% (aq), semiconductor grade, was purchased from J.T. Baker. Dry and degassed dichrolomethane and diethyl ether were obtained from an Innovative Technology solvent purification system and taken into an inert atmosphere glovebox in standard Schlenk glassware. Silicon wafers were purchased from Virginia Semiconductor with the following specifications: prime grade Si (100), single side polished, n-type, p-doped, thickness of 450 μm, and resistivity of 1−2 Ω·cm. All solvents were dried over alumina for 24 h twice and then passed through a fresh column of alumina prior to use.

Porous Silicon Preparation. 1.4 cm^2 (1.2 × 1.2 cm) wafer shards were cleaned by sonication (10 min in 1:1 acetone/ethanol) and rinsing with excess ethanol. Galvanostatic etching was performed using a 24.5% HF/25.5% H_2O/50% ethanol solution, using the silicon wafer with a heavy aluminum foil in contact with the unpolished side of the wafer (acting as the anode) and a Pt wire electrode (the cathode). The silicon was anodized at 7.6 mA cm^{-2} for 90 s and then 76 mA cm^{-2} for 120 s with full white-light illumination (~40 mW cm^{-2}) provided by an ELH bulb. The freshly etched samples were cleaned by rinsing with excess ethanol, followed by a brief soak in argon-sparged pentane and then dried with an argon stream and stored in a argon filled airtight glass vial in the dark.

DOI: 10.1021/jacs.5b05738
J. Am. Chem. Soc. 2015, 137, 9730−9738

Table 2. Representative Molecular Radical Reactions of Organochalcogenides

Entry	Molecular reaction	Reference(s)
1	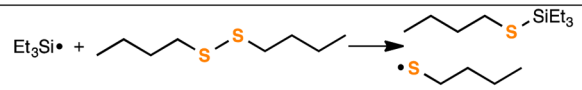	82
2	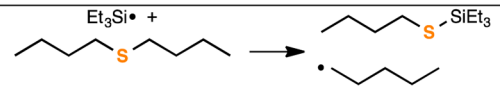	82
3	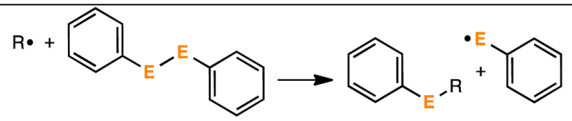	83-85
4	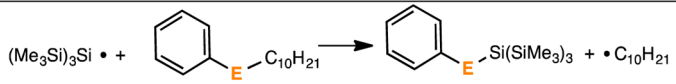	67
5	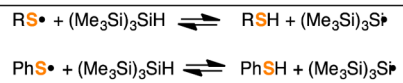	87-89

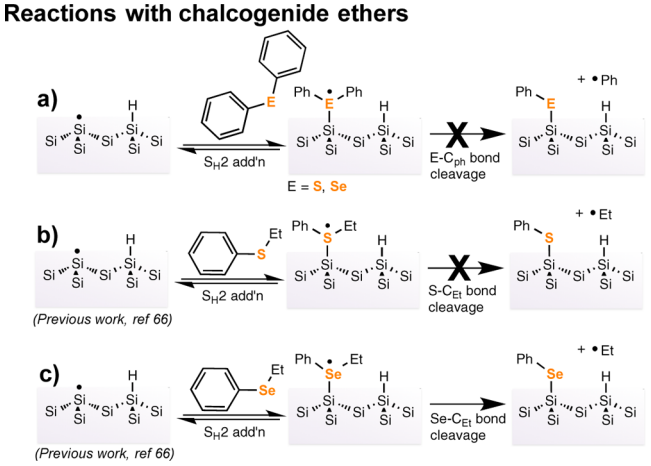

Figure 6. Proposed stepwise S_H2-based mechanism for chalcogenide ether reaction with silicon surface radicals. (a) Lack of reaction with diphenyl dichalcogenide (S, Se). (b) Lack of reaction of ethyl-phenylsulfide with a surface silicon radical (from previous work, ref 66). (c) Reaction of ethylphenylselenide with a surface silicon radical (from previous work, ref 66).

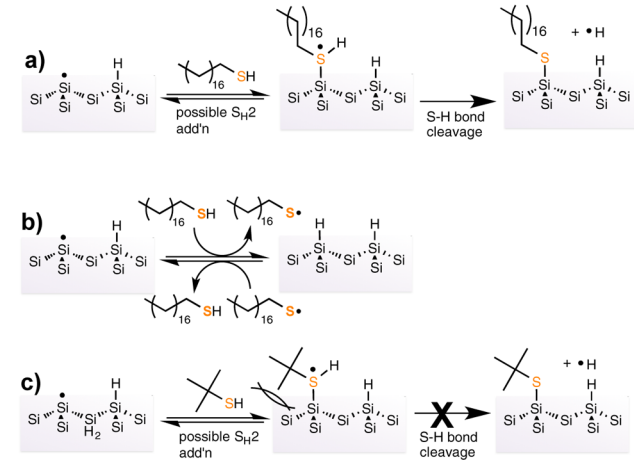

Figure 7. (a) Proposed reaction of an alkanethiol with a silicon surface radical; the mechanism shown here is a variant of the S_H2 reaction with chalcogenide ethers. (b) Equilibria between silyl and thiyl radicals. (c) Lack of reactivity of *t*-butylthiol, most likely due to steric interference.

Surface Reactions. All reactions, with the exception of the etching of porous silicon, were performed in the argon-filled glovebox. In preparation for surface reactivity, the following 100 mM solutions were prepared: BBD was dissolved in dry acetonitrile, diphenyl disulfide was dissolved in dry diethyl ether, and the remaining reagents, including 1-dodecene, were diluted with dry dichloromethane. Diphenyl disulfide was the only reagent with insufficient solubility in dichloromethane. These solutions were briefly sparged with nitrogen before passing over another alumina column just before use. 100 μL of the 100 mM solution of a specific reagent was added to a porous silicon substrate, followed 100 μL (100 mM) 4-bromodiazonium tetrafluoroborate and was allowed to react for 2 h in the dark. Reactions were carried out multiple times in an airtight glass vial or in the airtight Teflon cell, shown in the SI; airtight vessels were important to minimize solvent evaporation, as dry samples do not appear to react further. The Teflon cell doubled as an FTIR holder and was used for all samples analyzed by FTIR, and in particular for the % substitution reactions so that the same area of the porous silicon sample was analyzed by FTIR, before the reaction, and after the reaction. Slight differences in porous silicon film thickness could affect the results, and this approach minimizes this effect. Reactions were carried out in the dark. After 2 h of contact time, the silicon samples were rinsed three times with dry acetonitrile (with a stream from a pipet) and three times with dry dichloromethane to remove excess and unreacted reagents. The samples were then removed from the glovebox (sealed, to minimize air exposure), dried further under an argon stream, and then analyzed.

Analytical Techniques. FTIR spectra were collected on a Nicolet Nexus 760 spectrometer with a DTGS detector in a nitrogen-purged

DOI: 10.1021/jacs.5b05738
J. Am. Chem. Soc. 2015, 137, 9730−9738

sample chamber, with at least 512 scans with a resolution of 4 cm^{-1}. XPS was taken on a Kratos Axis 165 X-ray photoelectron spectrometer in the Alberta Centre for Surface Engineering and Science (ACSES). TOF-SIMS depth analysis was obtained on ToF−SIMS IV-100 (ION-TOF GmbH) at the Alberta Centre for Surface Engineering and Science (ACSES): The porous silicon sample was sputtered with a 1 kV Cs^+ ion source, leading to a 300 × 300 μm^2 crater with a central area of 120 × 120 μm^2.

■ ASSOCIATED CONTENT

Supporting Information

Raw FTIR spectra of functionalized porous silicon samples; representative FTIR spectra of the porous silicon surfaces treated with the five chalcogenides that did not react (as indicated in Figure 1), photographs of the reaction chambers, SEM image of the porous silicon. The Supporting Information is available free of charge on the ACS Publications website at DOI: 10.1021/jacs.5b05738.

■ AUTHOR INFORMATION

Corresponding Author

*jburiak@ualberta.ca

Notes

The authors declare no competing financial interest.

■ ACKNOWLEDGMENTS

We gratefully acknowledge support from the Canada Research Chairs program. Dr. Hosnay Mobarok is thanked for experimental assistance.

■ REFERENCES

(1) Peng, F.; Su, Y.; Zhong, Y.; Fan, C.; Lee, S. T.; He, Y. *Acc. Chem. Res.* **2014**, *47*, 612−623.
(2) Locritani, M.; Yu, Y.; Bergamini, G.; Baroncini, M.; Molloy, J. K.; Korgel, B. A.; Ceroni, P. *J. Phys. Chem. Lett.* **2014**, *5*, 3325−3329.
(3) Li, Y.; O'Leary, L. E.; Lewis, N. S.; Galli, G. *J. Phys. Chem. C* **2013**, *117*, 5188−5194.
(4) Lattimer, J. R. C.; Brunschwig, B. S.; Lewis, N. S.; Gray, H. B. *J. Phys. Chem. C* **2013**, *117*, 27012−27022.
(5) Vilan, A.; Yaffe, O.; Biller, A.; Salomon, A.; Kahn, A.; Cahen, D. *Adv. Mater.* **2010**, *22*, 140−159.
(6) Garg, K.; Majumder, C.; Nayak, S. K.; Aswal, D. K.; Gupta, S. K.; Chattopadhyay, S. *Phys. Chem. Chem. Phys.* **2015**, *17*, 1891−1899.
(7) Li, F.; Basile, V. M.; Pekarek, R. T.; Rose, M. J. *ACS Appl. Mater. Interfaces* **2014**, *6*, 20557−20568.
(8) Kuy, D.; Li, L.; Gao, Y.; Wang, C.; Jiang, J.; Xiong, Y. *Angew. Chem., Int. Ed.* **2015**, *54*, 2980−2985.
(9) Teplyakov, A. V.; Bent, S. F. *J. Vac. Sci. Technol., A* **2013**, *31*, 050810.
(10) Ciampi, S.; Harper, J. B.; Gooding, J. J. *Chem. Soc. Rev.* **2010**, *39*, 2158−2183.
(11) Gallant, B. M.; Gu, X. W.; Chen, D. Z.; Greer, J. R.; Lewis, N. S. *ACS Nano* **2015**, *9*, 5143−5153.
(12) Shi, L.; Harris, J. T.; Fenollosa, R.; Rodriguez, I.; Lu, X.; Korgel, B. A.; Meseguer, F. *Nature Commun.* **2013**, *4*, 1904.
(13) Higashi, G. S.; Chabal, Y. J.; Trucks, G. W.; Raghavachari, K. *Appl. Phys. Lett.* **1990**, *56*, 656−658.
(14) Higashi, G. S.; Becker, R. S.; Chabal, Y. J.; Becker, A. J. *Appl. Phys. Lett.* **1991**, *58*, 1656−1658.
(15) Thissen, P.; Seitz, O.; Chabal, Y. J. *Prog. Surf. Sci.* **2012**, *87*, 272−290.
(16) Newton, T. A.; Boiani, J. A.; Hines, M. A. *Surf. Sci.* **1999**, *430*, 67.
(17) Halimaoui, A. Porous Silicon Formation by Anodization. In *Properties of Porous Silicon*; Canham, L. T., Ed.; INSPEC: London, 1997; pp 12−23.
(18) Kim, N. Y.; Laibinis, P. E. *Inorganic Materials Synthesis, ACS Symposium Series*; ACS: Washington, DC, 2009; Vol *727*, pp 157−168.
(19) Morita, M.; Ohmi, T.; Hasegawa, E.; Kawakami, M.; Ohwada, M. *J. Appl. Phys.* **1990**, *68*, 1272.
(20) Steinrück, H.-G.; Schiener, A.; Schindler, T.; Will, J.; Magerl, A.; Konovalov, O.; Destri, G. L.; Seeck, O. H.; Mezger, M.; Haddad, J.; Deutsch, M.; Checco, A.; Ocko, B. M. *ACS Nano* **2014**, *8*, 12676−12681.
(21) Gusev, E. P.; Lu, H. C.; Gustafsson, T.; Garfunkel, E. *Phys. Rev. B: Condens. Matter Mater. Phys.* **1995**, *52*, 1759.
(22) Wong, K. T.; Lewis, N. S. *Acc. Chem. Res.* **2014**, *47*, 3037−3044.
(23) Chatterjee, P.; Hazra, S. *J. Phys. Chem. C* **2014**, *118*, 11350−11356.
(24) Linford, M. R.; Chidsey, C. E. D. *J. Am. Chem. Soc.* **1993**, *115*, 12631.
(25) Linford, M. R.; Fenter, P.; Eisenberger, P. M.; Chidsey, C. E. D. *J. Am. Chem. Soc.* **1995**, *117*, 3145.
(26) Sieval, A. B.; Demirel, A. L.; Nissink, J. W. M.; Linford, M. R.; van der Maas, J. H.; de Jeu, W. H.; Zuilhof, H.; Sudhölter, E. J. R. *Langmuir* **1998**, *14*, 1759.
(27) Li, Y.; Calder, S.; Yaffe, O.; Cahen, D.; Haick, H.; Kronik, L.; Zuilhof, H. *Langmuir* **2012**, *28*, 9920−9929.
(28) Buriak, J. M. *Chem. Rev.* **2002**, *102*, 1271−1308.
(29) Buriak, J. M. *Chem. Mater.* **2014**, *26*, 763−772.
(30) Liu, F.; Luber, E. J.; Huck, L. A.; Olsen, B. C.; Buriak, J. M. *ACS Nano* **2015**, *9*, 2184−2193.
(31) Rijksen, B.; Pujari, S. P.; Scheres, L.; van Rijn, C. J. M.; Baio, J. E.; Weidner, T.; Zuilhof, H. *Langmuir* **2012**, *28*, 6577−6588.
(32) Bélanger, D.; Pinson, J. *Chem. Soc. Rev.* **2011**, *40*, 3995−4048.
(33) Jaeckel, B.; Hunger, R.; Webb, L. J.; Jaegermann, W.; Lewis, N. S. *J. Phys. Chem. C* **2007**, *111*, 18204−18213.
(34) Segev, L.; Salomon, A.; Natan, A.; Cahen, D.; Kronik, L.; Amy, F.; Chan, C. K.; Kahn, A. *Phys. Rev. B* **2006**, *74*, 165323/1−165323/6.
(35) Hunger, R.; Fritsche, R.; Jaeckel, B.; Jaegermann, W.; Webb, L.; Lewis, N. *Phys. Rev. B: Condens. Matter Mater. Phys.* **2005**, *72*, 045317.
(36) Lopinski, G.; Eves, B.; Hul'ko, O.; Mark, C.; Patitsas, S.; Boukherroub, R.; Ward, T. *Phys. Rev. B: Condens. Matter Mater. Phys.* **2005**, *71*, 125308.
(37) Arefi, H. H.; Nolan, M.; Fagas, G. *J. Phys. Chem. C* **2015**, *119*, 11588−11597.
(38) Hacker, C. A. *Solid-State Electron.* **2010**, *54*, 1657−1664.
(39) Cooper, A. J.; Keyvanfar, K.; Deberardinis, A.; Pu, L.; Bean, J. C. *Appl. Surf. Sci.* **2011**, *257*, 6138−6144.
(40) Pujari, S. P.; van Andel, E.; Yaffe, O.; Cahen, D.; Weidner, T.; van Rijn, C. J. M.; Zuilhof, H. *Langmuir* **2013**, *29*, 570−580.
(41) Yaffe, O.; Pujari, S. P.; Sinai, O.; Vilan, A.; Zuilhof, H.; Kahn, A.; Kronik, L.; Cohen, H.; Cahen, D. *J. Phys. Chem. C* **2013**, *117*, 22422−22427.
(42) Arefi, H. H.; Fagas, G. *J. Phys. Chem. C* **2014**, *118*, 14346−14354.
(43) Lu, X.; Hessel, C. M.; Yu, Y.; Bogart, T. D.; Korgel, B. A. *Nano Lett.* **2013**, *13*, 3101−3105.
(44) McVey, B. F. P.; Tilley, R. D. *Acc. Chem. Res.* **2014**, *47*, 3045−3051.
(45) DeBenedetti, W. J.; Chiu, S.-K.; Radlinger, C. M.; Ellison, R. J.; Manhat, B. A.; Zhang, J. Z.; Shi, J.; Goforth, A. M. *J. Phys. Chem. C* **2015**, *119*, 9595−9608.
(46) Yang, Z.; De los Reyes, G. B.; Titova, L. V.; Sychogov, I.; Dasog, M.; Linnros, J.; Hegmann, F. A.; Veinot, J. G. C. *ACS Photonics* **2015**, *2*, 595−605.
(47) Dasog, M.; De los Reyes, G. B.; Titova, L. V.; Hegmann, F. A.; Veinot, J. G. C. *ACS Nano* **2014**, *8*, 9636−9648.
(48) Wheeler, L. M.; Neale, N. R.; Chen, T.; Kortshagen, U. R. *Nature. Comm.* **2013**, *4*, 2197.
(49) Zhou, T.; Anderson, R. T.; Li, H.; Bell, J.; Yang, Y.; Gorman, B. P.; Pylypenko, S.; Lusk, M. T.; Sellinger, A. *Nano Lett.* **2015**, *15*, 3657−3663.

DOI: 10.1021/jacs.5b05738
J. Am. Chem. Soc. 2015, 137, 9730−9738

(50) Balakumar, A.; Lysenko, A. B.; Carcel, C.; Malinovskii, V. L.; Gryko, D. T.; Schweikart, K. K. H.; Loewe, R. S.; Yasseri, A. A.; Liu, Z.; Bocian, D. F.; Lindsay, J. S. *J. Org. Chem.* **2004**, *69*, 1435−1443.
(51) Yasseri, A. A.; Syomin, D.; Loewe, R. S.; Lindsey, J. S.; Zaera, F.; Bocian, D. F. *J. Am. Chem. Soc.* **2004**, *126*, 15603−15612.
(52) Chatgilialoglu, C. *Chem. Rev.* **1995**, *95*, 1229−1251.
(53) Pandey, G.; Gadre, S. R. *Acc. Chem. Res.* **2004**, *37*, 201−210.
(54) Chatgilialoglu, C. *Chem. - Eur. J.* **2008**, *14*, 2310−2320.
(55) Hawari, J. A.; Griller, D.; Lossing, F. P. *J. Am. Chem. Soc.* **1986**, *108*, 3273−3275.
(56) Kachian, J. S.; Bent, S. F. *J. Am. Chem. Soc.* **2009**, *131*, 7005−7015.
(57) Coulter, S. K.; Schwartz, M. P.; Hamers, R. J. *J. Phys. Chem. B* **2001**, *105*, 3079−3087.
(58) Lai, Y.-H.; Yeh, C.-T.; Yeh, C.-C.; Hung, W.-H. *J. Phys. Chem. B* **2003**, *107*, 9351−9356.
(59) Zhu, Z.; Srivistava, A.; Osgood, R. M. *J. Phys. Chem. B* **2003**, *107*, 13939−13948.
(60) Kachian, J. S.; Tannaci, J.; Wright, R. J.; Tilley, T. D.; Bent, S. F. *Langmuir* **2011**, *27*, 179−186.
(61) Yu, L. H.; Gergel-Hackett, N.; Zangmeister, C. D.; Hacker, C. A.; Richter, C. A.; Kushmerick, J. G. *J. Phys.: Condens. Matter* **2008**, *20*, 374114.
(62) Lou, J. L.; Shiu, H. W.; Chang, L. Y.; Wu, C. P.; Soo, Y.-L.; Chen, C.-H. *Langmuir* **2011**, *27*, 3436−3441.
(63) Huang, Y.-S.; Chan, C.-H.; Chen, C.-H.; Hung, W.-H. *ACS Appl. Mater. Interfaces* **2013**, *5*, 5771−5776.
(64) Hacker, C. A. *Solid-State Electron.* **2010**, *54*, 1657−1664.
(65) Sano, H.; Ohno, K.; Ichii, T.; Murase, K.; Sugimura, H. *Jpn. J. Appl. Phys.* **2010**, *49*, 01AE09−1.
(66) Wang, D.; Buriak, J. M. *Langmuir* **2006**, *22*, 6214−6221.
(67) Ballestri, M.; Chatgilialoglu, C.; Clark, K. B.; Griller, D.; Giese, B.; Kopping, B. *J. Org. Chem.* **1991**, *56*, 678.
(68) Stewart, M. P.; Maya, F.; Kosynkin, D. M.; Dirk, S. M.; Stapleton, J. J.; McGuiness, C. L.; Allara, D. L.; Tour, J. M. *J. Am. Chem. Soc.* **2004**, *126*, 370.
(69) Huck, L. A.; Buriak, J. M. *J. Am. Chem. Soc.* **2012**, *134*, 489−497.
(70) de Smet, L. C. P. M; Zuilhof, H.; Sudh€olter, E. J. R.; Lie, L. H.; Houlton, A.; Horrocks, B. R. *J. Phys. Chem. B* **2005**, *109*, 12020.
(71) Buriak, J. M.; Stewart, M. J.; Geders, T. W.; Allen, M. J.; Choi, H. C.; Smith, J.; Raftery, M. D.; Canham, L. T. *J. Am. Chem. Soc.* **1999**, *121*, 11491−11502.
(72) Nemanick, E. J.; Hurley, P. T.; Webb, L. J.; Knapp, D. W.; Michalak, D. J.; Brunschwig, B. S.; Lewis, N. S. *J. Phys. Chem. B* **2006**, *110*, 14770−14778.
(73) Li, Y.; Buriak, J. M. *Inorg. Chem.* **2006**, *45*, 1096−1102.
(74) Girard, A.; Coulon, N.; Cardinaud, C.; Mohammed-Brahim, T.; Geneste, F. *Appl. Surf. Sci.* **2014**, *314*, 358−366.
(75) Nair, D. P.; Podgórski, M.; Chatani, S.; Gong, T.; Xi, W.; Fenoli, C. R.; Bowman, C. N. *Chem. Mater.* **2014**, *26*, 724−744.
(76) Dénès, F.; Pichowicz, M.; Povie, G.; Renaud, P. *Chem. Rev.* **2014**, *114*, 2587−2693.
(77) Subramanian, H.; Moorthy, R.; Sibi, M. P. *Angew. Chem., Int. Ed.* **2014**, *53*, 13660−13662.
(78) Renaud, P. Radical Reactions Using Selenium Precursors. In *Topics in Current Chemistry: Organoselenium Chemistry*; Springer-Verlag: Berlin, 2000; Vol *208*, pp 81−112.
(79) Bowman, W. R. Selenium Compounds in Radical Reactions. In *Organoselenium Chemistry: Synthesis and Reactions*; Wirth, T., Ed.; Wiley-VCH: Weinheim, 2011.
(80) Pandey, G.; Gadre, S. R. *Acc. Chem. Res.* **2004**, *37*, 201−210.
(81) Roberts, B. P. *Chem. Soc. Rev.* **1999**, *28*, 25−35.
(82) Soundarajan, N.; Jackson, J. E.; Platz, M. S. *J. Phys. Org. Chem.* **1988**, *1*, 39−46.
(83) Ogawa, A.; Doi, M.; Ogawa, I.; Hirao, T. *Angew. Chem., Int. Ed.* **1999**, *38*, 2027−2029.
(84) Russell, G. A.; Tashtoush, H. *J. Am. Chem. Soc.* **1983**, *105*, 1398−1399.
(85) Ogawa, A. Selenium and Tellerium in Organic Synthesis. In *Main Group Metals in Organic Synthesis*; Yamamoto, H., Oshima, K., Eds.; Wiley-VCH Verlag GmbH &Co. KGaA: Weinheim, 2003; Chapter 15.4, p 839.
(86) Nogueira, C. W.; Zeni, G.; Rocha, J. B. T. *Chem. Rev.* **2004**, *104*, 6225−6285.
(87) Wittenberg, D.; McNinch, H. A.; Gilman, H. *J. Am. Chem. Soc.* **1958**, *80*, 5418−5422.
(88) Chatgilialoglu, C. *Helv. Chim. Acta* **2006**, *89*, 2387−2398.
(89) Chatgilialoglu, C. *Chem. - Eur. J.* **2008**, *14*, 2310−2320.
(90) Zavitsas, A. A.; Chatgilialoglu, C. *J. Am. Chem. Soc.* **1995**, *117*, 10645−10654.
(91) The search for "hydrosilylation" and "surface" in Web of Science resulted in 1396 citations; the search for "hydrosilation" and "surface" in the same database resulted in 256 citations. One of the landmark papers in the field, ref 25 by Chidsey, has been cited 904 times according to Web of Science, 1085 times according to Google Scholar. Data as of July 7, 2015.

DOI: 10.1021/jacs.5b05738
J. Am. Chem. Soc. 2015, 137, 9730−9738